Cellulose (2014) 21:4569–4581
DOI 10.1007/s10570-014-0418-9

ORIGINAL PAPER

Production of highly electro-conductive cellulosic paper via surface coating of carbon nanotube/graphene oxide nanocomposites using nanocrystalline cellulose as a binder

Yanjun Tang · Zhibin He · Joseph Alexander Mosseler · Yonghao Ni

Received: 3 June 2014 / Accepted: 25 August 2014 / Published online: 29 August 2014

Abstract Electro-conductive cellulosic paper has attracted great attention as a promising alternative material in the emerging field of flexible and portable electronic devices. However, the environmentally friendly fabrication of electro-conductive cellulosic paper still remains challenging. Herein, green multi-walled carbon nanotube (MWCNT)/graphene oxide (GO) nanocomposites towards the sustainable development strategy were developed and subsequently used to impart electro-conductivity to cellulosic paper via surface coating process. GO exfoliated from graphite powder was used as a dispersant to improve the dispersion of MWCNTs in water media, and nanocrystalline cellulose (NCC) derived from cotton fibers was employed as a binder for the MWCNT/GO nanocomposites. Effect of NCC amount on the rheological behavior, particle size distribution, sedimentation stability and zeta potential of MWCNT/GO nanocomposites as well as the electro-conductivity and mechanical properties of coated paper was investigated. Results demonstrated that NCC enhanced the dispersion of MWCNT/GO nanocomposites in addition to serving as a binder. Surface coating application of MWCNT/GO nanocomposites was found to impart high electro-conductivity of up to 892 S m^{-1} to the cellulosic paper while improving its mechanical properties.

Keywords Electro-conductive cellulosic paper · Nanocrystalline cellulose · Multi-walled carbon nanotubes · Graphene oxide · Surface coating · Binders

Y. Tang (✉)
Key Laboratory of Advanced Textile Materials and Manufacturing Technology, Ministry of Education, Zhejiang Sci-Tech University, Hangzhou 310018, China
e-mail: tangyj@zstu.edu.cn

Y. Tang · Z. He · J. A. Mosseler · Y. Ni (✉)
Limerick Pulp and Paper Centre, University of New Brunswick, Fredericton E3B 5A3, Canada
e-mail: yonghao@unb.ca

Introduction

Cellulosic paper imparted with electro-conductivity, known as electro-conductive paper, inheriting its intrinsic properties such as flexibility, biocompatibility, light weight, low cost and recycling possibilities, has received considerable attention and shown great promise in such application areas as electrochromic displays, electroluminescent devices, chemical and electrochemical sensors, biosensors and membranes (Huang et al. 2005). In fact, cellulosic fiber itself is non-conductive. The electro-conductivity of cellulosic paper heavily depends on the nature of the electro-conductive fillers used and the production process. Currently, electro-conductive cellulosic paper may be manufactured using wet-end formation process and/or surface coating process. In practice, surface coating application provides significant commercial

advantages over the wet-end formation process, e.g., high filler retention, low cost and low-risk scale-up (Shen et al. 2010). Generally, the fillers used to impart electro-conductivity to cellulosic materials may include carbon black (Enríquez et al. 2012), carbon fiber (Jang and Ryu 2006), carbon nanotubes (CNTs) (Fugetsu et al. 2008; Imai et al. 2010; Oya and Ogino 2008) and graphene (Shateri-Khalilabad and Yazdanshenas 2013a, b), as well as polypyrrole (Ding et al. 2010; Qian et al. 2010; Wang et al. 2013) and polyaniline (Mao et al. 2014; Youssef et al. 2012). Among these electro-conductive fillers, CNTs are one of the most promising candidates due to their unique nanostructure and excellent physical properties (Ben-Valid et al. 2010; Qi et al. 2013). However, the inherent insolubility of CNTs in water media severely hinders their large scale use in related application fields (Kharissova et al. 2013; Richard et al. 2003).

To overcome this limitation, numerous efforts have been directed toward the surface engineering of CNTs for enhanced aqueous dispersion via covalent (Tagmatarchis et al. 2005) or non-covalent approach (Lee et al. 2007). As a matter of fact, surface modification can impair their inherently unique properties, thus affecting the end-use performance, although the aqueous dispersion was greatly improved (Zhang et al. 2010). Fortunately, graphene oxide (GO) used as a novel dispersant in aqueous system may solve the above mentioned problem (Tian et al. 2010). GO, a two-dimensional (2D) and one-atomic-thick sp^2 carbon layer exfoliated from graphite, shares many similar properties to CNTs (Zhao et al. 2012). Due to the hydrophilic oxygen-containing functional groups, GO can be readily dispersed in water media (Dreyer et al. 2010). Therefore, combining the CNTs and GO into CNT/GO nanocomposites is considered to be an effective route to improve the aqueous dispersion of CNTs and further extend their applications. Also, processing improvement of the CNT/GO nanocomposites/suspensions is the first step for their promising application in electro-conductive cellulosic paper.

In addition to the dispersant, binder is another essential component to satisfy the demands of surface coating (Rioux et al. 2011). Currently, the sustainable manufacturing strategy drives the demand for using biodegradable polymers as part of the wave of next generation materials (Shen and Fatehi 2013). For this reason, the application of lignocelluloses-derived chemicals/polymers is of great interest from academic research to industrial innovation because of their superior environmental and biological compatibility (Kurihara and Isogai 2014). In particular, nanocrystalline cellulose (NCC), a promising bio-based alternative to conventional petroleum-based polymers, has shown substantial potential in reinforcing conventional nanocomposites largely due to its unique characteristics, e.g., high tensile strength, high stiffness, high aspect ratio and a large surface area (Brinchi et al. 2013; Zaman et al. 2013). More importantly, NCC is dispersed in water media due to the presence of hydroxyl groups and sulfonic acid groups, which may offer a great potential for using NCC as a novel binder in CNT/GO nanocomposites. Also, optimization of NCC addition that can balance the electro-conductivity and mechanical properties of coated paper is of practical interest.

In the present work, surface coating of MWCNT/GO nanocomposites using NCC as a binder onto cellulosic substrate was proposed to produce electro-conductive paper. Significantly, this is the first time that green MWCNT/GO nanocomposites in combination with bio-based NCC were designed and subsequently employed to impart electro-conductivity to cellulosic paper. The scope of the study includes: (1) GO was exfoliated from raw graphite and used as a dispersant to improve the aqueous dispersion of MWCNTs; (2) NCC was isolated from cotton fibers via acid hydrolysis and employed as a binder for MWCNT/GO nanocomposites, the effects of NCC addition on the rheological behavior, particle size distribution, sedimentation stability and zeta potential of MWCNT/GO nanocomposites were investigated; (3) surface coating application of the resulting MWCNT/GO nanocomposites with various amounts of NCC for imparting electro-conductivity and improved mechanical properties to cellulosic paper was studied.

Experimental

Materials

Graphite powder (particle size <20 μm), multi-walled carbon nanotubes, sulfuric acid (H_2SO_4, 98 %), sodium carboxymethyl cellulose (CMC) (Molecular weight of 2,50,000 g mol^{-1} and DS of 0.90),

hydrochloric acid (HCl, 37 %), potassium permanganate ($KMnO_4$), sodium nitrate ($NaNO_3$), hydrogen peroxide (H_2O_2, 30 %) and sodium hydroxide (NaOH) were purchased from Aldrich-Sigma. Carboxylated styrene butadiene (SB) latex with a solid content of 50 % was received from Dow Chemical Company. Commercial paper made of recycled fibers, with a thickness of 245 μm, was supplied by a paper mill in Eastern Canada and used as substrates for surface coating process. Deionized water was used for all experiments.

Preparation of NCC

The preparation of rod-shaped NCC from cotton material followed a similar procedure as described in our recent work (Tang et al. 2014). Briefly, cotton fibers were initially ground to pass through a 0.85 mm screen in a Wiley mill. Then, 10 g of ground powder was gradually added into 110 mL of 64.0 wt% sulfuric acid aqueous solution. The hydrolysis was run at 45 °C for 90 min with continuous stirring. Afterwards, deionized water was added to terminate the hydrolysis. Subsequently, the resulting mixture was centrifuged at 11,000 rpm for 10 min to separate the nanocellulose, which was then washed with deionized water and repeatedly centrifuged for 4 times. The obtained colloidal suspension of nanocellulose was filtered with deionized water in a dialysis bag for a whole day to a constant pH of 7.0. Eventually, the suspensions underwent freeze drying and vacuum drying prior to the subsequent processing.

Preparation of GO

The GO sample was prepared from graphite powder by following the modified Hummers method (Hummers and Offeman 1958; Li et al. 2013). Typically, 10 g of graphite powder together with 5 g of $NaNO_3$ were added to 230 mL of H_2SO_4, and the mixture was magnetically stirred for 1 h in an ice/water bath. Then, 30 g of $KMnO_4$ was gradually added into the above mixture and the reaction was allowed to continue for 2 h in the ice/water bath. Afterward, the reaction was further continued with stirring for 36 h at 40 °C. Subsequently, deionized water was added to dilute the mixture to 1,000 mL, followed by adding 200 mL of H_2O_2 (5 %). The mixture was centrifuged at 4,000 rpm for 30 min and then washed first with 5 % HCl solution and then with deionized water (three times). Finally, the suspension was dried and thus GO was successfully obtained.

Preparation of MWCNT/GO nanocomposites

The GO sample was firstly dispersed in deionized water under stirring using an electrical agitator (IKA T25) at 10,000 rpm for 10 min, followed by the addition of MWCNTs. The weight ratio of MWCNTs to GO was 4:1. The mixture was first stirred for 20 min at 15,000 rpm and then sonicated (Qsonica Q1376, USA) for 10 min at 1,000 W and 20 kHz in an ice/water bath to form aqueous suspensions. Afterward, various amounts (based on total dry weight of MWCNTs and GO) of NCC at 4.0, 6.0, 8.0, 10.0, 12.0 and 14.0 wt% used as a binder were dispersed in the above suspensions for 20 min at 12,000 rpm to obtain the targeted MWCNT/GO nanocomposites with a solid content of 5 wt% by weight. Eventually, the pH of the MWCNT/GO nanocomposites was adjusted to about 7.5. In addition, for FTIR and XRD analysis, a small portion of nanocomposites was further poured in a polytek mold and dried in an oven at 40 °C for 8 h to form nanocomposite films. To better understand the role of NCC in improving the electro-conductivity of MWCNT/GO nanocomposite coated paper, MWCNTs suspensions and GO suspensions were prepared in the presence of 6 wt% of NCC, respectively. More importantly, typical MWCNT/GO nanocomposites were prepared for comparison purpose using carboxylated styrene butadiene (SB) latex, a conventional binder, instead of NCC. Unlike the added NCC, the required addition of SB latex was 16 wt% for satisfying the requirements of coating process (Lehtinen 2000).

Preparation of coated paper

Prior to surface coating process, the commercial paper made of recycled fibers underwent a surface sizing process with CMC solution (mass concentration of 0.5 %) in order to minimize the water penetration. The sizing weight was controlled at 2 ± 0.1 g/m^2, and the contact angle of deionized water to the CMC-sized - paper was at 74°. The CMC-sized paper was then the base paper for surface coating process in the subsequent work. The surface sizing and coating process were performed using the Meyer rod coating set-up (K303,

RK Print Coat Instruments Ltd, UK). Coated paper was prepared by applying the MWCNT/GO nanocomposites to the surface of base paper with a Meyer bar, which allowed for a uniform coating thickness of 20 ± 2 μm. Eventually, coated paper was subject to vacuum drying (Isotemp 285A) at 80 °C for 24 h.

Dispersion measurement of MWCNT/GO nanocomposites

The viscosity of MWCNT/GO nanocomposites was measured (Brookfield viscometer, USA) using # 4 spindle at a shear force (speed) range of 1.5–100 rpm. The MWCNT/GO nanocomposites with various amounts of NCC were stirred for 10 min at 10,000 rpm, shaken (Burrel., Model 75) for 20 min, followed by ultrasonic dispersion (Bransonic, 3510R-DTH, 100 W) for 5 min, and finally set for 24 h prior to measurement on a UV–Vis spectrophotometer (Milton Roy, 1001 Plus) at 500 nm. The hydrodynamic particle size distribution and distribution averages for the MWCNT/GO nanocomposites with and without NCC addition were determined using a zeta potential analyzer (Zetaplus, Brookhaven Instruments Cooperation) equipped with 90 plus/BI-MASS software. The size measurements were carried out at 25 °C at a scattering angle of 90° (Sun et al. 2014). The first order result from the dynamic light scattering (DLS) experiments is an intensity distribution of particle sizes, which is naturally weighted according to the scattering intensity of each fraction or family, and can then be converted to a volume/mass distribution. The Zeta potential was calculated by measuring the electrophoretic mobility using the same instrument. Data were acquired in the phase analysis light scattering (PALS) mode following solution equilibration at 25 °C. Calculation of zeta potential from the measured nanoparticle electrophoretic mobility employed the Smoluchowski Equation, as detailed in an early reference (Pan et al. 2003). All data were averaged of 6 cycles with 10 scans for each.

Characterization and analysis

MWCNT, GO, NCC and MWCNT/GO nanocomposites were re-dispersed in deionized water and then placed on an ultra-thin carbon-coated copper grid, followed by drying under an infrared lamp. A JSM-2100 transmission electron microscopy (TEM, JEOL, Japan) setup at an accelerating voltage of 80 kV was used. Fourier-transformed infrared (FTIR) spectra of MWCNT/GO nanocomposite film samples was performed on a Nicolet 5700 spectrometer (Thermo Fisher Scientific, USA) with a resolution of 4 cm^{-1} at the range of 4,000–400 cm^{-1}, the samples were palletized with KBr powder. X-ray diffraction (XRD) patterns of MWCNT/GO nanocomposite film samples were recorded on a diffractometer (X'TRA-055, ARL, Switzerland) at 40.0 kV and 120 mA with Cu K-alpha radiation.

X-ray diffraction data were collected from $2\theta = 5$–60° at a scan rate of 2°/min. The base paper and coated paper samples were conditioned at 23 °C and 50 % RH for 24 h prior to the measurement of mechanical properties. The basis weight and thickness of base paper were first determined, and the weight and thickness of the paper after surface coating were subsequently measured, according to TAPPI methods T-410 and T-411, respectively. The coat weight and coating thickness were separately calculated by the difference of the above two measurements. The mechanical measurements including breaking length (667, L&W) and tearing strength (B-2115, L&W) of based paper and coated paper followed TAPPI methods T-404 and T-414, respectively. Electro-conductivity of coated paper was measured using the two-probe method on a model 2750 multimeter/switch system (Keithley). Coated paper samples were cut into strips (15 mm width). Two samples were prepared under each condition, and the electro-conductivity was measured 3 times at different spots on the surface, the average of these 6 results was reported. The electro-conductivity (S/m) of coated paper was calculated according to Eq. (1) (Kamyshny et al. 2011; Saravanan et al. 2014):

$$\sigma = 1/\rho = L/R \cdot d \cdot h \tag{1}$$

where ρ is resistivity in ohm meter (Ω m), R is the measured resistance of a conductor (Ω), d is the width of paper strips (m), h is the coating thickness (m), and L is the distance between the two probes (m).

Results and discussion

Proposed process concept of surface coating of MWCNT/GO nanocomposites for imparting high electro-conductivity to cellulosic paper.

Our strategy for the fabrication of highly electro-conductive cellulosic paper via surface coating of MWCNT/GO nanocomposites is illustrated in Scheme 1. GO exfoliated from graphite contains abundant hydroxyl groups in addition to carbonyl and carboxyl groups, due to the applied strongly oxidative conditions. These oxygen-containing functionalities alter the van der Waals interactions between the layers of GO and render them hydrophilic, thus facilitating their hydration and exfoliation in aqueous media (Zhang et al. 2010). In the current study, GO was used as a dispersant for the hydrophobic MWCNTs. Furthermore, NCC isolated from cotton fibers via acid hydrolysis, was employed as an effective binder for the aqueous processing of MWCNT/GO nanocomposites. In addition, surface coating process provides an attractive route for the application of MWCNT/GO nanocomposites onto paper surface to yield the desired high electro-conductivity.

Overall, the reaction and processing of MWCNT/GO nanocomposites were carried out in water media rather than organic systems, which fit well into the sustainable manufacturing strategy. Moreover, both the MWCNT/GO nonocomposites and the targeted electro-conductive cellulosic paper were composed entirely of recyclable carbon-based and bio-based materials, which can be considered as green materials.

Effect of NCC addition on the rheological behavior of MWCNT/GO nanocomposites

Rheological behavior measurement is an effective approach to predict the performance of composites in the potential application, particularly in industrial paper coating process (Nisogi et al. 2000). In reality, the information derived from rheological behavior measurements plays an important role in the production of surface coated paper (Tang et al. 2013). Herein, the shear rheological behavior of MWCNT/GO nanocomposites as a function of various amounts of NCC was determined, and the results are shown in Fig. 1.

As can be seen, all MWCNT/GO nanocomposite samples showed a typical shear-thinning behavior within the shear rate range of 1.5–100 rpm. However, the incorporation of NCC led to a pronounced change in rheological behavior of MWCNT/GO nanocomposites. The viscosity increased with the amount of NCC added. Specifically, in the absence of NCC,

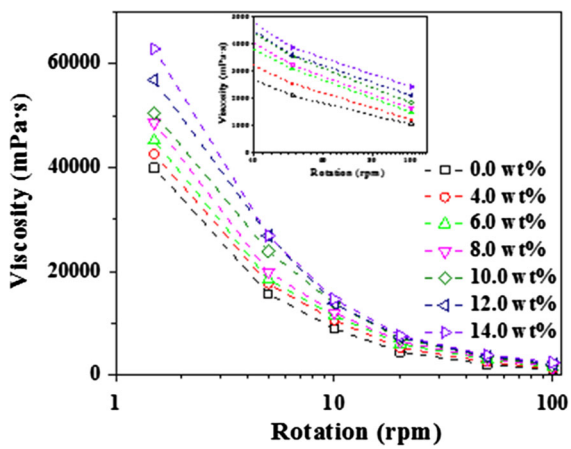

Fig. 1 Effect of NCC addition on the rheological behavior of MWCNT/GO nanocomposites (The weight ratio of MWCNTs to GO was 4:1, solid content of 5 wt%, pH of 7.5)

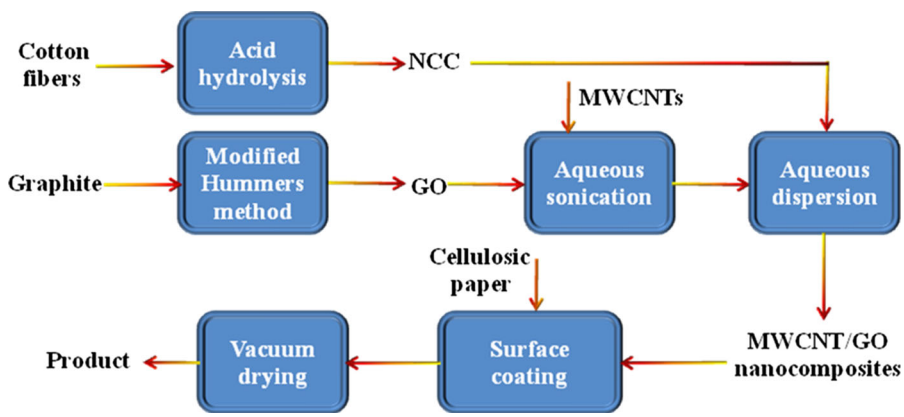

Scheme 1 Schematic illustration of surface coating of MWCNT/GO nanocomposites to produce highly electro-conductive cellulosic paper

MWCNT/GO nanocomposites exhibited a viscosity of 1,040 mPa s at 100 rpm, at 4.0 wt% of NCC, the viscosity increased to 1,220 mPa s, and further to 1,490, 1,640 mPa s at 6.0, 8.0 wt% of NCC, respectively, implying that NCC acted as an effective thickening agent in these MWCNT/GO nanocomposites. The increased viscosity of MWCNT/GO nanocomposites as a function of increased NCC concentration may be explained by the fact that NCC interacted strongly with water because of its inherent high polarity and large surface area, acting to form a highly entangled network exhibiting its well-known gel-like behavior, therefore leading to the increased resistance to flow (Dimic-Misic et al. 2013; Mohtaschemi et al. 2014). It was noted that the MWCNT/GO nanocomposites possessed a viscosity of 2,120 mPa s at 12.0 wt% of NCC. With further increasing the amount of NCC, the viscosity still maintained a steady uptrend. As a rule, in industrial paper coating process, it is preferred that the Brookfield viscosity would be in a range of 1,000–2,000 mPa s at 100 rpm (Lehtinen 2000). Based on this consideration, the added amount of NCC should not be higher than 10.0 wt% under the condition studied.

Effect of NCC addition on the dispersion of MWCNT/GO nanocomposites

Surface anionic cellulose nanofibrils may have nanodispersing effects on the CNTs in water (Koga et al. 2013). In one study (Olivier et al. 2012), highly stable single-walled carbon nanotube (SWCNT) dispersions were achieved after ultrasonication in cellulose nanocrystal (CN) aqueous colloidal suspensions. The improved dispersion was considered to be due to the short-range hydrophobic interactions between the SWCNTs and specific crystalline faces of the CNs and the long-range electrostatic repulsion between the CNs. In another study (Koga et al. 2013), TEMPO-oxidized cellulose nanofibrils (TOCNs) were found to effectively improve the dispersion of SWCNTs in water, presumably due to a CH-π interaction between the axial plane of the cellulose and the graphene π-conjugated system. Here, in addition to serving as a binder, NCC may be also expected to improve the dispersion of MWCNT/GO nanocomposites (Boluk et al. 2012). The average particle size and particle size distribution of MWCNT/GO nanocomposites as a function of the NCC addition were determined, and the results are shown in Fig. 2. The original NCC suspensions exhibited an average particle size of

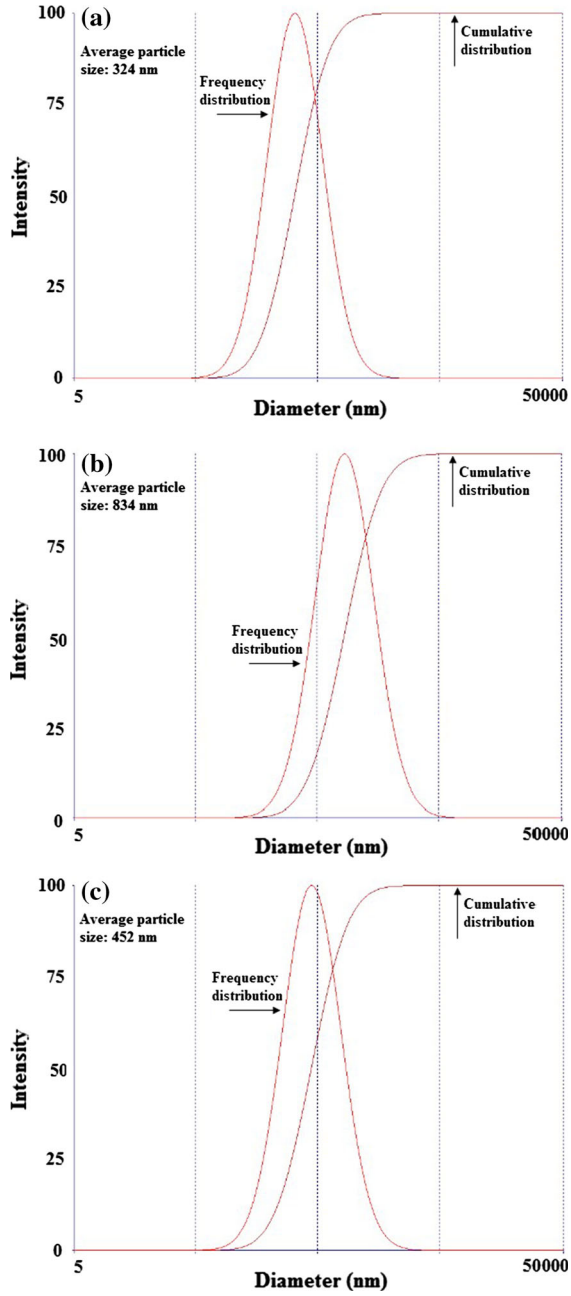

Fig. 2 Particle size distribution and average particle size of **a** NCC suspensions, as well as MWCNT/GO nanocomposites **b** without NCC and **c** with 4.0 wt% of NCC (All measurements were conducted in aqueous solutions with solid content of 1 mg/mL at pH 7.5 and 25 °C, the weight ratio of MWCNTs to GO was 4:1)

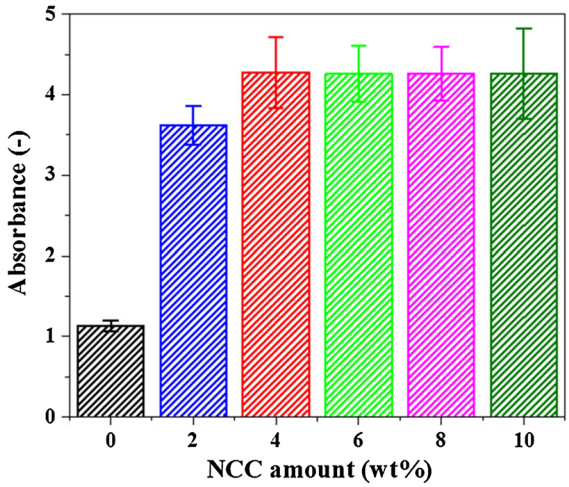

Fig. 3 UV–Vis absorbance at 500 nm of the MWCNT/GO nanocomposites as a function of various amounts of NCC (Solid content of 1 wt%, the weight ratio of MWCNTs to GO was 4:1, pH of 7.5, storage for 24 h)

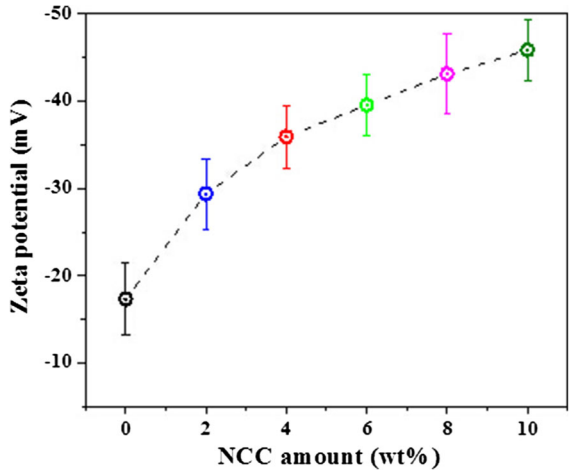

Fig. 4 Zeta potential of MWCNT/GO nanocomposites as a function of various amounts of NCC addition (All measurements were performed in aqueous solutions with solid content of 1 mg/mL at pH 7.5 and 25 °C, the weight ratio of MWCNTs to GO was 4:1)

324 nm (Fig. 2a), in good agreement with that reported in a previous study (Fan and Li 2012). In the absence of NCC, the MWCNT/GO nanocomposites displayed a particle size distribution within a range of 50–5,000 nm and had an average particle size of 834 nm (Fig. 2b). Whereas, the addition of 4.0 wt% of NCC improved the dispersion of the MWCNT/GO nanocomposites, and its average particle size decreased to 452 nm (Fig. 2c), which is very close to the average particle size of MWCNTs modified by ionic-complementary peptides (Sheikholeslam et al. 2012).

Furthermore, the UV–Vis absorbance measurements were conducted to evaluate the role of NCC amount on the sedimentation stability of MWCNT/GO nanocomposites. As shown in Fig. 3, in the absence of NCC, the absorbance of the MWCNT/GO nanocomposites was 1.13. Evidently, the added amount had a marked effect on the sedimentation stability. Specifically, at 2 wt% of NCC, the absorbance of the MWCNT/GO nanocomposites reached 3.62, which increased to 4.28 at 4 wt% of NCC. With further increasing the NCC amount, the absorbance remained almost unchanged. Therefore, it can be concluded that the NCC addition can facilitate the dispersion of MWCNT and GO nanocomposites in water media.

Moreover, the zeta potential was also measured as a function of the NCC addition, as presented in Fig. 4. The zeta potential of the MWCNT/GO nanocomposites without NCC was −17.35 mV, in agreement with that reported in an early study for MWCNT suspensions at pH 7.5 (−18.50 mv) (Sheikholeslam et al. 2012). The NCC absorbed on the surface of GO and MWCNT can endow the nanocomposites with more negative charges due to the abundant sulfonic groups of NCC. With the increase of NCC addition from 4.0 to 8.0 wt%, the zeta potential exhibited increasingly electronegative from −29.36 to −35.88 mV, which further changed to −45.86 at 10.0 wt% of NCC addition. The increased zeta potential may be partially responsible for the improved dispersion of MWCNT/GO nanocomposites as discussed above.

TEM analysis of MWCNT/GO nanocomposites

Figure 5a and b demonstrate the morphology change from graphite to GO. It is evident that graphite possessed multi-layer structures with deep color, while the applied strong oxidation imparted the GO with one or two light-colored layer structure, similar to that reported in the literature (Krishnamoorthy et al. 2013; Veerapandian et al. 2012). Figure 5c reveals that MWCNTs exhibited structures with diameters of approximately 20 nm and lengths ranging from 1 to 5 μm. The morphology of

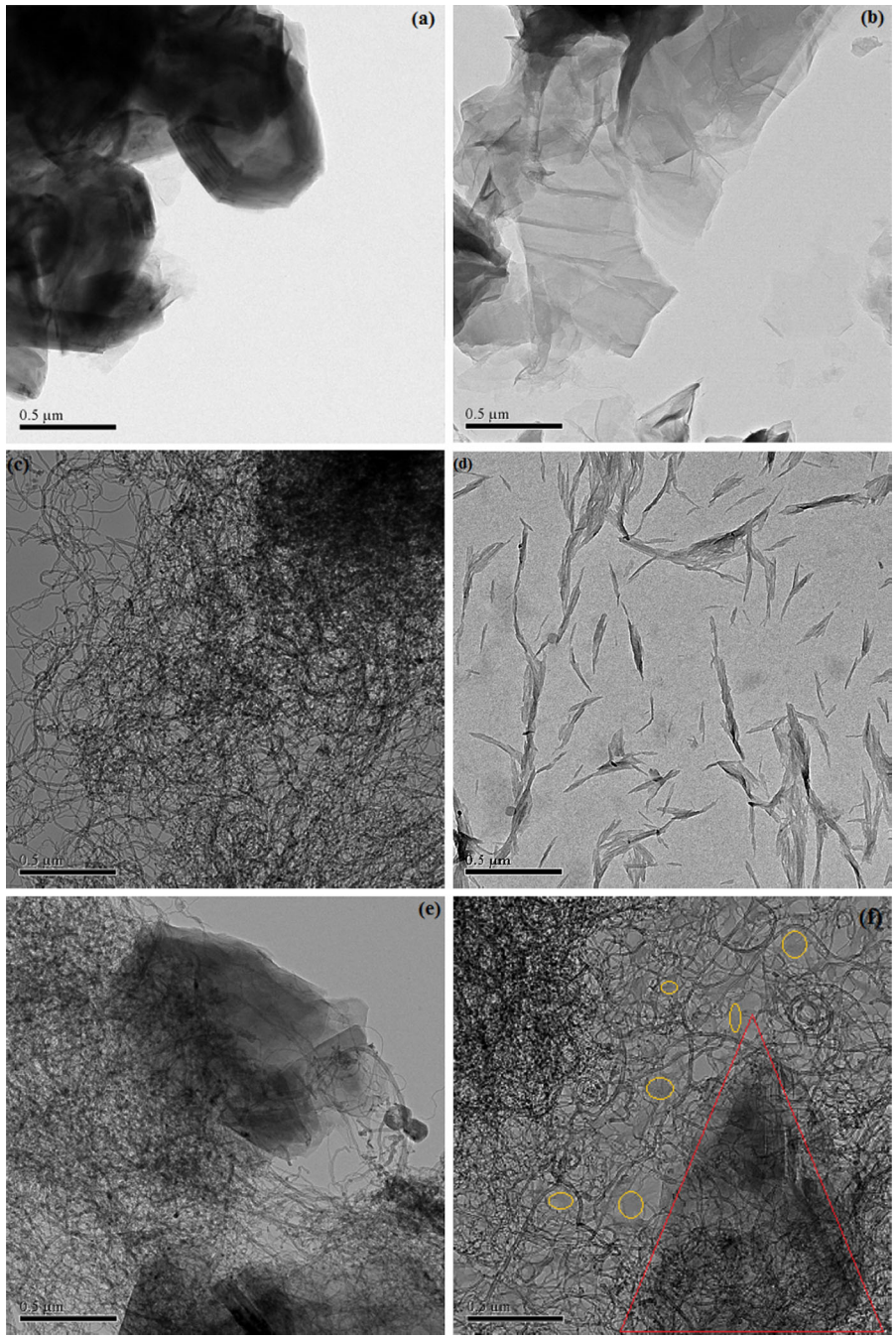

Fig. 5 TEM images of **a** graphite, **b** GO, **c** MWCNTs, **d** NCC, as well as MWCNT/GO nanocomposites **e** without NCC and **f** with 4.0 wt% of NCC

NCC is shown in Fig. 5d. It exhibited rod-shaped structures with widths of 10–30 nm and lengths of 100–300 nm. The TEM images of MWCNT/GO nanocomposites without and with 4.0 wt% of NCC, are compared in Fig. 5e and f. In the presence of NCC (the yellow circles in Fig. 5f), the exfoliated GO sheets were completely covered by MWCNTs (the red triangle in Fig. 5f), so that an interconnected network between

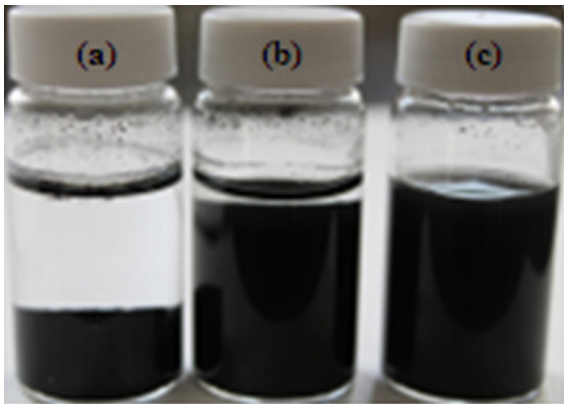

Fig. 6 Digital images of **a** pristine MWCNT suspensions, as well as MWCNT/GO nanocomposites **b** without NCC and **c** with 4.0 wt% of NCC (Solid content 1 wt%, the weight ratio of MWCNTs to GO was 4:1, pH of 7.5, storage for 24 h)

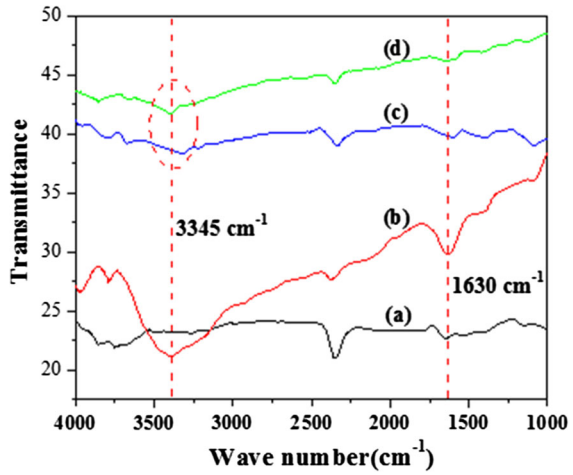

Fig. 7 FTIR spectra of **a** MWCNTs, **b** GO, as well as MWCNT/GO nanocomposite film **c** without NCC and **d** with 4.0 wt% of NCC

MWCNTs and GO sheets can be formed. It can be suggested that the presence of NCC greatly contributed to the emulsification of MWCNT/GO nanocomposites, further facilitating the interaction between MWCNTs and GO sheets.

More importantly, as illustrated in Fig. 6, the pristine MWNTs can not form stable suspensions in water even after a long time sonication, thus leading to serious precipitation and aggregation. Whereas, the incorporation of GO significantly altered the dispersion state of CNTs in water media. The presence of NCC had a positive effect on further improving the dispersion stability.

FTIR spectra of MWCNT/GO nanocomposites

FTIR spectra of (a) MWCNTs, (b) GO, as well as MWCNT/GO nanocomposite films (c) without and (d) with 4.0 wt% of NCC are shown in Fig. 7. It can be observed that a broad absorption band occurred at 3,345 cm^{-1} in spectrum (b), which was associated with the stretching vibration of hydroxyl groups of GO. Furthermore, a strong peak at 1,630 cm^{-1} can be attributed to the stretching vibration of carbonyl groups (Zhang et al. 2010). In the FTIR spectra of the MWNT/GO nanocomposite films (Spectrum c, d, without and with NCC, respectively), it is apparent that the broad absorption band related to the hydroxyl groups (3,345 cm^{-1}) and the carbonyl groups (1,630 cm^{-1}) are present, supporting the presence of GO in the MWCNT/GO nanocomposite films, since these oxygen-containing functional groups are from the GO sample but are absent in the MWCNTs sample (Spectrum a).

XRD analysis of MWCNT/GO nanocomposites

XRD patterns of (a) MWCNTs, (b) GO, as well as MWCNT/GO nanocomposite films (c) without and (d) with NCC are illustrated in Fig. 8. MWCNT exhibited the typical peak of 002 at 2θ of 26° (curve a), which is in good agreement with the previously reported result (Shen et al. 2014). For GO, a typical diffraction peak at 2θ of 12° can be observed (curve b), corresponding to the diffraction of (002) plane (Yuan et al. 2012). In contrast to the XRD pattern of MWCNT and GO, MWCNT/GO nanocomposite films displayed the corresponding peaks at 2θ of 12° and 26° (curve c), respectively, possibly due to the adsorption and intercalation of the MWCNT on GO sheets. In addition, the presence of NCC appeared to exert limited effect on the XRD pattern of MWCNT/GO nanocomposite films. The sample with NCC showed the XRD pattern (curve d) similar to that of the nanocomposite films without NCC.

Effect of NCC addition on the electro-conductivity and mechanical properties of coated paper

Largely owing to the superior environmental and biological compatibility in addition to the unique

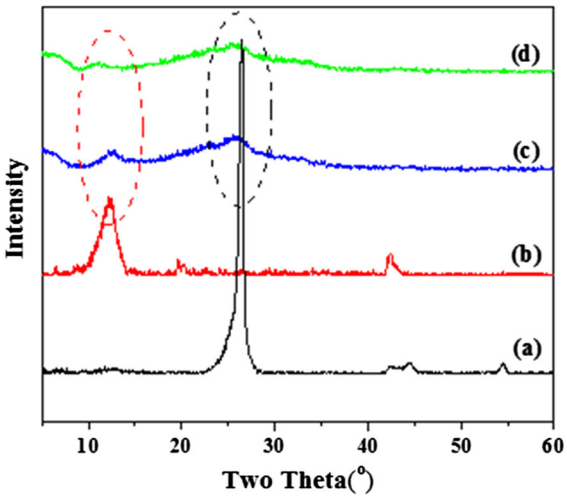

Fig. 8 XRD patterns of **a** MWCNTs, **b** GO, as well as MWCNT/GO nanocomposite films **c** without NCC and **d** with 4.0 wt% of NCC

interfacial properties, the application of nanoscale lignocelluloses-derived chemicals as a coating agent in paper production is of great practical interest (Fatehi 2013). For instance, to determine the potential of nanofibrillated cellulose (NFC) for use as a coating material, the characteristics of several NFC-coated samples on a synthetic fiber sheet were studied (Hamada and Bousfield 2010). Besides, a small amount of cellulose nanofibers (the weight ratio of cellulose nanofibers to PCC varied in the range of 1–5 %) was found to be effective in binding PCC particles onto the filter paper substrate when dip coated on its surface (Arbatan et al. 2012). Here, a series of MWCNT/GO nanocomposites with different amounts of NCC were coated on the surface of a low-grade paper made of recycled fibers with the objective of imparting high electro-conductivity and improved mechanical properties to cellulosic paper. Besides, the effects of MWCNTs suspensions and GO suspensions as well as the MWCNT/GO nanocomposites with SB latex on the final properties of coated paper were also investigated.

As shown in Table 1, the optimal amount of NCC in MWCNT/GO nanocomposites that imparted the highest electro-conductivity to the coated paper, was 6.0 wt%, which yielded the electro-conductivity of 892 S m^{-1}. This is caused by (a) the non-electro-conductive nature of NCC, (b) improvement of the MWCNT/GO conductive network due to the NCC binding effect. Using the conventional latex (SB) as the binder, instead of NCC, the electro-conductivity was 156 S m^{-1}. It should be noted that the coated paper exhibited a very high electro-conductivity (up to 892 S m^{-1}), based on those reported in the literature where CNTs were used in wet-end formation process (Anderson et al. 2010 (3 S m^{-1}); Fugetsu et al. 2008 (189 S m^{-1}); Imai et al. 2010 (671 S m^{-1}); Jung et al. 2008 (0.21 S m^{-1}) or poly (3,4-ethylenedioxythiophene) was applied in surface coating process [Kawashima et al. 2012 (180 S m^{-1})]. On the other hand, compared to MWCNT/GO nanocomposites, MWCNTs suspensions and GO suspensions imparted lower electro-conductivities

Table 1 Effect of NCC addition on the electro-conductivity and mechanical properties of coated paper

Sample ID	Electro-conductivity (S m^{-1})	Breaking length (km)		Tearing strength (mN)	
		MD	CD	MD	CD
Base paper	$\ll 10^{-10}$	6.08 ± 0.24	2.44 ± 0.16	1,242 ± 17	1,497 ± 36
CMC-sized paper	$\ll 10^{-10}$	6.30 ± 0.17	2.54 ± 0.10	1,263 ± 24	1,526 ± 41
MWCNT/GO/NCC-coated paper					
NCC-4.0 wt%	679 ± 43	6.02 ± 0.32	2.40 ± 0.09	1,198 ± 58	1,458 ± 64
NCC-6.0 wt%	892 ± 35	6.43 ± 0.44	2.52 ± 0.20	1,287 ± 19	1,522 ± 91
NCC-8.0 wt%	551 ± 51	6.79 ± 0.38	2.61 ± 0.22	1,345 ± 61	1,584 ± 72
NCC-10.0 wt%	282 ± 62	7.21 ± 0.30	2.76 ± 0.14	1,405 ± 78	1,596 ± 55
MWCNT/GO/SB-coated paper	156 ± 13	6.39 ± 0.28	2.55 ± 0.17	1,276 ± 42	1,529 ± 69
MWCNT/NCC-coated paper	595 ± 47	6.11 ± 0.22	2.38 ± 0.16	1,224 ± 37	1,462 ± 49
GO/NCC-coated paper	105 ± 18	7.35 ± 0.55	2.72 ± 0.19	1,420 ± 44	1,614 ± 47

MD machine direction, represents the direction of paper which is run along the track of paper machine, *CD* cross direction, means the direction of paper which is run vertical upright to the grain of the paper

(595, 105 S m^{-1}, respectively) to coated paper at 6 wt% of NCC addition, implying that a synergistic effect of CNTs and GO on the electro-conductivity of coated paper may be expected, as shown in Table 1.

In addition, the balance between the electro-conductivity and mechanical properties of coated paper was considered, as also shown in Table 1. In general, MWCNT, GO and NCC, components of the obtained nanocomposites, have shown great promise in reinforcing the conventional industrial materials due to their inherently excellent mechanical properties. The real concern in reinforcing the coated paper lies in the interaction between these novel materials and cellulosic fiber networks (Fatehi et al. 2010). Similarly, the mechanical resistance of the MWCNT/GO nanocomposites against peeling is particularly important for surface coating applications. In this sense, being a binder, NCC may play a decisive role in enhancing the mechanical properties of coated paper. To verify the assumption, effect of NCC amount on the breaking length and tearing strength of coated paper was investigated, and the results are also shown in Table 1. The breaking length in machine direction (MD) and cross direction (CD) of the base paper was 6.08 and 2.44 km, respectively. The paper surface sized with CMC exhibited an increase in breaking length. Furthermore, the mechanical properties of the paper coated by MWCNT/GO nanocomposites were largely controlled by the added NCC amount. With a sufficient amount of NCC addition, (6–10 wt% NCC on the MWCNT/GO nanocomposites) the mechanical properties of resulting paper was improved. Specifically, at 8, 10 wt% NCC on the MWCNT/GO nanocomposites, the breaking length in MD of coated paper reached 6.79, 7.21 km, showing percentage increases of 11.68, 18.59, respectively, in comparison with that of base paper. Similar improvement in the tearing strength was also observed.

Conclusion

Based on sustainable manufacturing strategy, green MWCNT/GO nanocomposites useful in imparting electro-conductivity to coated paper were successfully fabricated by using NCC as a binder. It was found that the added NCC increased the viscosity and zeta potential, decreased the average particle size and improved the sedimentation stability of MWCNT/GO nanocomposites. Furthermore, FTIR and XRD results confirmed that MWCNTs and GO underwent sufficient interaction to form the resulting nanocomposites. Upon surface coating of the MWCNT/GO nanocomposites, a low-grade paper made of recycled fibers was imparted with electro-conductivities of up to 892 S m^{-1}. Meanwhile, the mechanical properties of the cellulosic paper were enhanced after surface coating. With the easy scale-up procedure, environmental compatibility and good performance, this novel electro-conductive cellulosic paper holds potential for practical applications in portable electronics and future generations of flexible electronic devices.

Acknowledgments This work was financially supported by a NSERC CRD grant (CRDPJ 363811-07), Canada Research Chairs programs of the Government of Canada, the National Natural Science Foundation of China (Grant No. 31100442), Zhejiang Provincial Natural Science Foundation of China (Grant No. LY14C160003) and 521 Talent Cultivation Program of Zhejiang Sci-Tech University (Grant No. 11110132521310).

References

Anderson RE, Guan J, Ricard M, Dubey G, Su J, Lopinski G, Dorris G, Bourne O, Simard B (2010) Multifunctional single-walled carbon nanotube-cellulose composite paper. J Mater Chem 20(12):2400–2407

Arbatan T, Zhang L, Fang X, Shen W (2012) Cellulose nanofibers as binder for fabrication of superhydrophobic paper. Chem Eng J 210:74–79

Ben-Valid S, Botka B, Kamarás K, Zeng A, Yitzchaik S (2010) Spectroscopic and electrochemical study of hybrids containing conductive polymers and carbon nanotubes. Carbon 48(10):2773–2781

Boluk Y, Zhao L, Incani V (2012) Dispersions of nanocrystalline cellulose in aqueous polymer solutions: structure formation of colloidal rods. Langmuir 28(14):6114–6123

Brinchi L, Cotana F, Fortunati E, Kenny JM (2013) Production of nanocrystalline cellulose from lignocellulosic biomass: technology and applications. Carbohydr Polym 94(1):154–169

Dimic-Misic K, Puisto A, Gane P, Nieminen K, Alava M, Paltakari J, Maloney T (2013) The role of MFC/NFC swelling in the rheological behavior and dewatering of high consistency furnishes. Cellulose 20(6):2847–2861

Ding C, Qian X, Yu G, An X (2010) Dopant effect and characterization of polypyrrole-cellulose composites prepared by in situ polymerization process. Cellulose 17(6):1067–1077

Dreyer DR, Park S, Bielawski CW, Ruoff RS (2010) The chemistry of graphene oxide. Chem Soc Rev 39(1):228–240

Enríquez E, Fernández JF, de la Rubia MA (2012) Highly conductive coatings of carbon black/silica composites obtained by a sol–gel process. Carbon 50(12):4409–4417

Fan J, Li Y (2012) Maximizing the yield of nanocrystalline cellulose from cotton pulp fiber. Carbohydr Polym 88(4): 1184–1188

Fatehi P (2013) Recent advancements in biorefinery: from biomass to bioproduct and biofuel. Curr Orgc Chem 17(15):1569

Fatehi P, Liu X, Ni Y, Xiao H (2010) Interaction of cationic modified poly vinyl alcohol with high yield pulp. Cellulose 17(5):1021–1031

Fugetsu B, Sano E, Sunada M, Sambongi Y, Shibuya T, Wang X, Hiraki T (2008) Electrical conductivity and electromagnetic interference shielding efficiency of carbon nanotube/cellulose composite paper. Carbon 46(9): 1256–1258

Hamada H, Bousfield DW (2010) Nanofibrillated cellulose as a coating agent to improve print quality of synthetic fiber sheets. Tappi J 9(11):25–29

Huang B, Kang GJ, Ni Y (2005) Preparation of conductive paper by in situ polymerization of pyrrole in a pulp fiber system. Pulp Paper Can 107:38–41

Hummers WS Jr, Offeman RE (1958) Preparation of graphitic oxide. J Am Chem Soc 80(6):1339

Imai M, Akiyama K, Tanaka T, Sano E (2010) Highly strong and conductive carbon nanotube/cellulose composite paper. Compos Sci Technol 70(10):1564–1570

Jang J, Ryu SK (2006) Physical property and electrical conductivity of electroless Ag-plated carbon fiber-reinforced paper. J Mater Proc Technol 180(1):66–73

Jung R, Kim HS, Kim Y, Kwon SM, Lee HS, In HJ (2008) Electrically conductive transparent papers using multiwalled carbon nanotubes. J Polym Sci, Part B: Polym Phys 46(12):1235–1242

Kamyshny A, Steinke J, Magdassi S (2011) Metal-based inkjet inks for printed electronics. Open Appl Phys J 4(1):19–36

Kawashima H, Shinotsuka M, Nakano M, Goto H (2012) Fabrication of conductive paper coated with PEDOT: preparation and characterization. J Coat Technol Res 9(4):467–474

Kharissova OV, Kharisov BI, de Casas Ortiz EG (2013) Dispersion of carbon nanotubes in water and non-aqueous solvents. RSC Adv 3(47):24812–24852

Koga H, Saito T, Kitaoka T, Nogi M, Suganuma K, Isogai A (2013) Transparent, conductive, and printable composites consisting of TEMPO-oxidized nanocellulose and carbon nanotube. Biomacromolecules 14(4):1160–1165

Krishnamoorthy K, Veerapandian M, Yun K, Kim S (2013) The chemical and structural analysis of graphene oxide with different degrees of oxidation. Carbon 53:38–49

Kurihara T, Isogai A (2014) Properties of poly(acrylamide)/TEMPO-oxidized cellulose nanofibril composite films. Cellulose 21(1):291–299

Lee JU, Huh J, Kim KH, Park C, Jo WH (2007) Aqueous suspension of carbon nanotubes via non-covalent functionalization with oligothiophene-terminated poly (ethylene glycol). Carbon 45(5):1051–1057

Lehtinen E (2000) Pigment coating and surface sizing of paper, Papermaking Science and Technology Series Book 11. Helsinki Univ Technol, Fapet Oy

Li S, Zhao W, Wang J, Qian L, Wang K, Pan M (2013) Synthesis and characterization of the thin paper-like graphite oxide and graphene. J Wuhan Univ Technol 35(1):1–6

Mao H, Wu X, Qian X, An X (2014) Conductivity and flame retardancy of polyaniline-deposited functional cellulosic paper doped with organic sulfonic acids. Cellulose 21(1): 697–704

Mohtaschemi M, Dimic-Misic K, Puisto A, Korhonen M, Maloney T, Paltakari J, Alava M (2014) Rheological characterization of fibrillated cellulose suspensions via bucket vane viscometer. Cellulose 21(3):1305–1312

Nisogi H, Bousfield DW, Lepoutre PF (2000) Influence of coating rheology on final coating properties. Tappi J 83(2): 100–106

Olivier C, Moreau C, Bertoncini P, Bizot H, Chauvet O, Cathala B (2012) Cellulose nanocrystal-assisted dispersion of luminescent single-walled carbon nanotubes for layer-by-layer assembled hybrid thin films. Langmuir 28(34):12463–12471

Oya T, Ogino T (2008) Production of electrically conductive paper by adding carbon nanotubes. Carbon 46(1):169–171

Pan D, Turner JL, Wooley KL (2003) Folic acid-conjugated nanostructured materials designed for cancer cell targeting. Chem Commun 19:2400–2401

Qi H, Mäder E, Liu J (2013) Electrically conductive aerogels composed of cellulose and carbon nanotubes. J Mater Chem A 1(34):9714–9720

Qian X, Chen J, An X (2010) Polypyrrole-coated conductive paper prepared by vapour-phase deposition method. Appita J 63(2):102–107

Richard C, Balavoine F, Schultz P, Ebbesen TW, Mioskowski C (2003) Supramolecular self-assembly of lipid derivatives on carbon nanotubes. Science 300(5620):775–778

Rioux R, Bousfield DW, Triantafillopoulos N (2011) A study of the mechanical properties of coated papers using elastica stiffness and low-load indentation. Tappi J 10(10):41–48

Saravanan C, He Z, Ni Y (2014) Application of polyaniline/clay combination to cellulosic paper as an approach to conductivity development. Bioresources 9(2):1886–1897

Shateri-Khalilabad M, Yazdanshenas ME (2013a) Preparation of superhydrophobic electroconductive graphene-coated cotton cellulose. Cellulose 20(2):963–972

Shateri-Khalilabad M, Yazdanshenas ME (2013b) Fabricating electroconductive cotton textiles using graphene. Carbohydr Polym 96(1):190–195

Sheikholeslam M, Pritzker M, Chen P (2012) Dispersion of multiwalled carbon nanotubes in water using ionic-complementary peptides. Langmuir 28(34):12550–12556

Shen J, Fatehi P (2013) A review on the use of lignocellulose-derived chemicals in wet-end application of papermaking. Curr Org Chem 17(15):1647–1654

Shen J, Song Z, Qian X, Ni Y (2010) A review on use of fillers in cellulosic paper for functional applications. Ind Eng Chem Res 50(2):661–666

Shen XJ, Pei XQ, Liu Y, Fu SY (2014) Tribological performance of carbon nanotube–graphene oxide hybrid/epoxy composites. Compos B 57:120–125

Sun B, Hou Q, Liu Z, He Z, Ni Y (2014) Stability and efficiency improvement of ASA in internal sizing of cellulosic paper by using cationically modified cellulose nanocrystals. Cellulose 21(2):2879–2887

Tagmatarchis N, Zattoni A, Reschiglian P, Prato M (2005) Separation and purification of functionalised water-soluble multi-walled carbon nanotubes by flow field-flow fractionation. Carbon 43(9):1984–1989

Tang Y, Zhou D, Zhang J, Zhu X (2013) Fabrication and properties of paper coatings with the incorporation of nanoparticle pigments: rheological behavior. Dig J Nanomater Biostruct 8(4):1699–1710

Tang Y, Yang S, Zhang N, Zhang J (2014) Preparation and characterization of nanocrystalline cellulose via low-intensity ultrasonic-assisted sulfuric acid hydrolysis. Cellulose 21(1):335–346

Tian L, Meziani MJ, Lu F, Kong CY, Cao L, Thorne TJ, Sun Y (2010) Graphene oxides for homogeneous dispersion of carbon nanotubes. ACS Appl Mater Interfaces 2(11): 3217–3222

Veerapandian M, Lee M, Krishnamoorthy K, Yun K (2012) Synthesis, characterization and electrochemical properties of functionalized graphene oxide. Carbon 50(11): 4228–4238

Wang H, Leaukosol N, He Z, Fei G, Si C, Ni Y (2013) Microstructure, distribution and properties of conductive polypyrrole/cellulose fiber composites. Cellulose 20(4): 1587–1601

Youssef AM, El-Samahy MA, Abdel Rehim MH (2012) Preparation of conductive paper composites based on natural cellulosic fibers for packaging applications. Carbohydr Polym 89(4):1027–1032

Yuan NY, Ma FF, Fan Y, Liu YB, Ding JN (2012) High conductive ethylene vinyl acetate composites filled with reduced graphene oxide and polyaniline. Compos A Appl Sci Manufact 43(12):2183–2188

Zaman M, Liu H, Xiao H, Chibante F, Ni Y (2013) Hydrophilic modification of polyester fabric by applying nanocrystalline cellulose containing surface finish. Carbohydr Polym 91(2):560–567

Zhang C, Ren L, Wang X, Liu T (2010) Graphene oxide-assisted dispersion of pristine multiwalled carbon nanotubes in aqueous media. J Phys Chem C 114(26):11435–11440

Zhao M, Liu X, Zhang Q, Tian G, Huang J, Zhu W, Wei F (2012) Graphene/single-walled carbon nanotube hybrids: one-step catalytic growth and applications for high-rate Li-S batteries. ACS Nano 6(12):10759–10769